Ion-ion collision dynamics in two-dimensional Cartesian space

M. S. Pindzola
Department of Physics, Auburn University, Auburn, Alabama 36849
(Received 18 January 2000; published 15 August 2000)

Ion-ion collision dynamics are studied by direct solution of the time-dependent Schrödinger and Dirac equations on a two-dimensional Cartesian lattice. The time-dependent Dirac equation is solved in both its two- and four-component forms using difference offsetting on the lattice to mitigate the fermion doubling pathology. For Pd^{46+} on Pd^{45+}, which energetically corresponds to U^{92+} on U^{91+} in a three-dimensional space, total inelastic probabilities are calculated at a fixed ion velocity and several impact parameters. In this intermediate energy range, the total inelastic probabilities from the Schrödinger and two- and four-component Dirac equations are in reasonable agreement, although the detailed collision dynamics reveal interesting differences.

PACS number(s): 34.50.−s

I. INTRODUCTION

Collisions between highly charged atomic ions provide an interesting test of relativistic scattering theory in the presence of strong electromagnetic fields. One of the most promising nonperturbative approaches is the direct solution of the time-dependent Dirac equation on a numerical lattice [1]. With the continuing development of more powerful computing platforms, the numerical feasibility of making extensive scattering calculations using time-dependent lattice methods is now dawning. An early formulation solved the time-dependent Dirac equation at zero impact parameter using two-dimensional cylindrical coordinates on a finite difference lattice for collisions of Ca^{20+} on U^{91+} [2] and U^{92+} on U^{91+} [3,4]. Subsequent work solved the time-dependent Dirac equation at nonzero impact parameters using three-dimensional Cartesian coordinates on a basis spline lattice to extract muon pair production cross sections for collisions of Au ions [5,6] and U ions [7] and electron pair production cross sections for collisions of U^{92+} on Au^{78+} [8].

By domain decomposition over a distributed-memory parallel computer, we have recently solved the time-dependent Schrödinger equation in three-dimensional Cartesian coordinates and extracted state-selective excitation and charge-transfer cross sections for proton-hydrogen [9,10] and proton-lithium [11] collisions. In this paper we extend those same lattice techniques to the solution of the time-dependent Dirac equation for ion-ion collisions. To reduce computational demands in our exploratory studies and yet retain the concept of an impact parameter, we first consider ion-ion collisions in two-dimensional Cartesian space. In previous work on proton-hydrogen [12] and antiproton-hydrogen [13] collisions using the time-dependent Schrödinger equation, we have found that the scattering dynamics in two-dimensional space is in good qualitative agreement with that found in full three-dimensional calculations.

We solve the time-dependent Dirac equation in both its two- and four-component forms on a two-dimensional lattice. The two-component form has been used in field-theoretical studies of quantum gravity [14], of particles obeying fractional statistics [15], and of spontaneously broken gauge theories [16]. The two-component form has recently been used to study the planar hydrogen atom in a strong magnetic field [17]. The four-component form has been favored in studies of intense laser-atom dynamics [18,19]. For either form, we solve the time-dependent Dirac equation using difference offsetting on the lattice to mitigate the fermion doubling pathology [20–23]. The ground-state binding energy in two-dimensional space is four times that found in three-dimensional space. Thus, we carry out lattice calculations for collisions of Pd^{46+} on Pd^{45+}, which energetically corresponds to U^{92+} on U^{91+} in full three dimensions. To check our relativistic calculations we choose an intermediate energy and solve the time-dependent Schrödinger equation in two dimensions for the same collision partners. As a final check, we increase the radial spacing between lattice points and solve the four-component time-dependent Dirac equation on a three-dimensional lattice for one impact parameter. In Sec. II we review collision theory involving the time-dependent Schrödinger and Dirac equations in two- and three-dimensional space, computational lattice results are presented in Sec. III, and a brief summary is given in Sec. IV. For simplicity, conventional three-dimensional atomic units are used throughout the paper (i.e., 1.0 hartree = 27.212 eV).

II. THEORY

The time-dependent Schrödinger equation in two spatial dimensions for a bare ion (Z_p) projectile colliding with a hydrogenic ion (Z_t) target is given by

$$i\frac{\partial\Psi(x,y,t)}{\partial t}=\left(-\frac{1}{2}\frac{\partial^2}{\partial x^2}-\frac{1}{2}\frac{\partial^2}{\partial y^2}-\frac{Z_t}{r}-\frac{Z_p}{r'(t)}\right)\Psi(x,y,t), \tag{1}$$

where

$$r=\sqrt{x^2+y^2}, \tag{2}$$

$$r'(t)=\sqrt{(x-b)^2+[y-(y_0+vt)]^2}, \tag{3}$$

b is the impact parameter, and v is the projectile velocity for straight line motion parallel to the y axis beginning at (b,y_0) with $y_0<0$.

The time-dependent Dirac equation in two spatial dimensions is given by

$$i\frac{\partial\vec{\Psi}(x,y,t)}{\partial t}=\left(-ic\alpha_x\frac{\partial}{\partial x}-ic\alpha_y\frac{\partial}{\partial y}-\frac{Z_t}{r}-\frac{G_LZ_p}{r''(t)}+\beta c^2\right)\times\vec{\Psi}(x,y,t), \tag{4}$$

where

$$r''(t)=\sqrt{(x-b)^2+\gamma^2[y-(y_0+vt)]^2}, \tag{5}$$

c is the speed of light, and $\gamma=1/\sqrt{1-(v^2/c^2)}$. The factor G_L in the projectile potential is given in the Lorentz gauge by [1]

$$G_L=\gamma\left(1-\frac{v}{c}\alpha_y\right). \tag{6}$$

The two-component form of the Dirac equation is obtained by choosing the Dirac matrices equal to the standard Pauli matrices:

$$\alpha_x=\begin{pmatrix}0&1\\1&0\end{pmatrix},\quad \alpha_y=\begin{pmatrix}0&-i\\i&0\end{pmatrix},\quad \beta=\begin{pmatrix}1&0\\0&-1\end{pmatrix}. \tag{7}$$

We find the two-component Dirac equation to be covariant under Lorentz transformations in three-dimensional spacetime (one time, two space). The standard nonrelativistic reduction of Eq. (4) yields

$$i\frac{\partial\Psi_L(x,y,t)}{\partial t}=\left(-\frac{1}{2}\frac{\partial^2}{\partial x^2}-\frac{1}{2}\left[\frac{\partial}{\partial y}+\frac{i}{c}A_y\right]^2-\frac{Z_t}{r}-\frac{Z_p}{r'(t)}+\frac{1}{2c}\frac{\partial A_y}{\partial x}\right)\Psi_L(x,y,t), \tag{8}$$

where

$$A_y=\frac{\beta Z_p}{r'(t)}, \tag{9}$$

and Ψ_L is the ''large'' component of the $\vec{\Psi}$ spinor.

The four-component form of the Dirac equation is obtained by choosing only three of the four Dirac matrices:

$$\alpha_x=\begin{pmatrix}0&0&0&1\\0&0&1&0\\0&1&0&0\\1&0&0&0\end{pmatrix},\quad \alpha_y=\begin{pmatrix}0&0&1&0\\0&0&0&-1\\1&0&0&0\\0&-1&0&0\end{pmatrix},$$

$$\beta=\begin{pmatrix}1&0&0&0\\0&1&0&0\\0&0&-1&0\\0&0&0&-1\end{pmatrix}. \tag{10}$$

The four-component Dirac equation is also found to be covariant under Lorentz transformations in three-dimensional spacetime. The standard nonrelativistic reduction of Eq. (4) now yields

$$i\frac{\partial}{\partial t}\begin{pmatrix}\Psi_{L1}(x,y,t)\\\Psi_{L2}(x,y,t)\end{pmatrix}=\left(-\frac{1}{2}\frac{\partial^2}{\partial x^2}-\frac{1}{2}\left[\frac{\partial}{\partial y}+\frac{i}{c}A_y\right]^2-\frac{Z_t}{r}-\frac{Z_p}{r'(t)}\right)\begin{pmatrix}\Psi_{L1}(x,y,t)\\\Psi_{L2}(x,y,t)\end{pmatrix} \tag{11}$$

$$+\frac{1}{2c}\begin{pmatrix}0&i\\-i&0\end{pmatrix}\frac{\partial A_y}{\partial x}\begin{pmatrix}\Psi_{L1}(x,y,t)\\\Psi_{L2}(x,y,t)\end{pmatrix}, \tag{12}$$

where $\binom{\Psi_{L1}}{\Psi_{L2}}$ is the ''large'' spinor component of the $\vec{\Psi}$ bispinor.

The exact analytic solution for the ground state of the Schrödinger equation in two dimensions is given by

$$\psi_{1s}^{\rm ex}(x,y)=\sqrt{\frac{8Z_t^2}{\pi}}e^{-2Z_tr}, \tag{13}$$

with

$$E_{1s}=-2Z_t^2. \tag{14}$$

To provide a proper representation of the ground state on our choice of two-dimensional lattice, we relax the exact analytic solution by solving the time-dependent Schrödinger equation in imaginary time ($\tau=it$):

$$-\frac{\partial\psi_{1s}(x,y)}{\partial\tau}=\left(-\frac{1}{2}\frac{\partial^2}{\partial x^2}-\frac{1}{2}\frac{\partial^2}{\partial y^2}-\frac{Z_t}{r}\right)\psi_{1s}(x,y). \tag{15}$$

The exact analytic solution for the ground state of the two-component Dirac equation in two dimensions is given by

$$\vec{\psi}_{1s}^{\rm ex}(x,y)=\sqrt{\frac{\eta_1\eta}{\pi\Gamma(1+2\delta)(\eta_1+\eta_2)}}\frac{(2\eta r)^\delta}{\sqrt{r}}e^{-\eta r}\times\begin{pmatrix}1\\-\frac{\eta_2}{\eta}e^{-i\theta}\end{pmatrix}, \tag{16}$$

with

$$\delta=\sqrt{\frac{1}{4}-\left(\frac{Z_t}{c}\right)^2} \tag{17}$$

and

$$E_{1s}=-(1-2\delta)c^2. \tag{18}$$

In Eq. (16), $\eta_1=(1+2\delta)c$, $\eta_2=(1-2\delta)c$, and $\eta=\sqrt{\eta_1\eta_2}$. The exact analytic solution for the ground state of the four-component Dirac equation in two dimensions is given by

$$\vec{\psi}_{1s}^{\rm ex}(x,y)=\sqrt{\frac{\eta_1\eta}{\pi\Gamma(1+2\delta)(\eta_1+\eta_2)}}\frac{(2\eta r)^{\delta}}{\sqrt{r}}e^{-\eta r}\times\begin{pmatrix}1\\0\\i\frac{\eta_2}{\eta}\cos\theta\\i\frac{\eta_2}{\eta}\sin\theta\end{pmatrix},\tag{19}$$

and the energy E_{1s} is the same as found in Eq. (18). We relax the exact analytic solution by solving the time-dependent ''squared'' Dirac equation in imaginary time:

$$-\frac{\partial\vec{\psi}_{1s}(x,y)}{\partial\tau}=\left(-ic\alpha_x\frac{\partial}{\partial x}-ic\alpha_y\frac{\partial}{\partial y}-\frac{Z_t}{r}+\beta c^2\right)^2\vec{\psi}_{1s}(x,y).\tag{20}$$

We solve the time-dependent Schrödinger and Dirac equations using lattice techniques to obtain a discrete representation of the wave function $[\vec{\psi}(x,y)\rightarrow\vec{\psi}_{i,j}]$ and all operators on a two-dimensional Cartesian mesh. Local operators, such as the potential energy, become diagonal matrices composed of their values at the lattice points $[V(x,y)\rightarrow V_{i,j}]$. Derivative operators, such as the kinetic energy, have lattice representations in terms of banded matrices. The spatial derivatives in the Schrödinger equation may be given by standard central difference formulas [24]:

$$\frac{\partial^2\psi(x,y)}{\partial x^2}\rightarrow\frac{\psi_{i+1,j}-2\psi_{i,j}+\psi_{i-1,j}}{\Delta x^2},\tag{21}$$

or

$$\frac{\partial^2\psi(x,y)}{\partial x^2}\rightarrow\frac{-\psi_{i+2,j}+16\psi_{i+1,j}-30\psi_{i,j}+16\psi_{i-1,j}-\psi_{i-2,j}}{12\Delta x^2},\tag{22}$$

where Δx is the lattice spacing. To avoid the fermion doubling pathology, the spatial derivatives in the Dirac equation may be given by standard backward-forward difference formulas [24]:

$$\frac{\partial\psi_u(x,y)}{\partial x}\rightarrow\frac{3\psi_{i,j}-4\psi_{i-1,j}+\psi_{i-2,j}}{2\Delta x},\qquad\frac{\partial\psi_l(x,y)}{\partial x}\rightarrow\frac{-\psi_{i+2,j}+4\psi_{i+1,j}-3\psi_{i,j}}{2\Delta x},\tag{23}$$

or

$$\frac{\partial\psi_u(x,y)}{\partial x}\rightarrow\frac{3\psi_{i+1,j}+10\psi_{i,j}-18\psi_{i-1,j}+6\psi_{i-2,j}-\psi_{i-3,j}}{12\Delta x},\tag{24}$$

$$\frac{\partial\psi_l(x,y)}{\partial x}\rightarrow\frac{\psi_{i+3,j}-6\psi_{i+2,j}+18\psi_{i+1,j}-10\psi_{i,j}-3\psi_{i-1,j}}{12\Delta x},$$

where the subscripts u,l refer to the upper positive and lower negative energy components of $\vec{\psi}(x,y)$.

Following Bottcher and Strayer [21], central differences for the spatial derivatives in the one-dimensional free-particle Dirac equation lead to bivalued energy dispersion relations. The three- and five-point central difference dispersion relations are given by

$$E^2=\left(\frac{1-\cos 2p\Delta x}{2\Delta x^2}\right)c^2+c^4\tag{25}$$

and

$$E^2=\left(\frac{130-32\cos p\Delta x-128\cos 2p\Delta x+32\cos 3p\Delta x-2\cos 4p\Delta x}{144\Delta x^2}\right)c^2+c^4,\tag{26}$$

where p is the linear momentum and $p_0=\pi/\Delta x$ is the maximum momentum on the lattice. The three- and five-point backward-forward differences found in Eqs. (23) and (24) lead to the following energy dispersion relations:

$$E^2=\left(\frac{13-16\cos p\Delta x+3\cos 2p\Delta x}{2\Delta x^2}\right)c^2+c^4\tag{27}$$

and

$$E^2=\left(\frac{470-528\cos p\Delta x+48\cos 2p\Delta x+16\cos 3p\Delta x-6\cos 4p\Delta x}{144\Delta x^2}\right)c^2+c^4.\tag{28}$$

In Fig. 1 we compare the four approximate energy dispersion relations with the exact result: $E^2=p^2c^2+c^4$ for $\Delta x=0.001$. The symmetric three- and five-point central difference dispersion relations associate a single energy to two different momenta. The offset three- and five-point backward-forward difference dispersion relations are single valued, and thus not subject to the fermion doubling pathology.

For implementation on distributed-memory parallel computers, the two-dimensional lattice is partitioned over processors along the y axis. Message passing between processors is restricted to lattice points at the partition boundaries needed to evaluate first or second derivatives in y. Relaxation in imaginary time uses a power series expansion of the exponential operator in the expression

$$\psi(\tau+\Delta\tau)=e^{-\Delta\tau H}\psi(\tau), \tag{29}$$

while propagation in real time uses a second-order differencing scheme:

$$\Psi(t+\Delta t)=\Psi(t-\Delta t)-2i\Delta t H\Psi(t). \tag{30}$$

In either case, the matrix-vector multiplications needed are performed in parallel.

The total inelastic probability at a specific incident velocity and impact parameter is given by

$$\wp_{\text{inelastic}}(v,b)=1-\left|\int dx\int dy\,\psi_{1s}^{*}(x,y)\Psi(x,y,T)\right|^2, \tag{31}$$

where

$$\Psi(x,y,0)=\psi_{1s}(x,y), \tag{32}$$

and $\Psi(x,y,T)$ is the solution of Eq. (1) at a time T following the collision. The total inelastic ''cross section'' is given by

$$\sigma_{\text{inelastic}}(v)=2\int \wp(v,b)db. \tag{33}$$

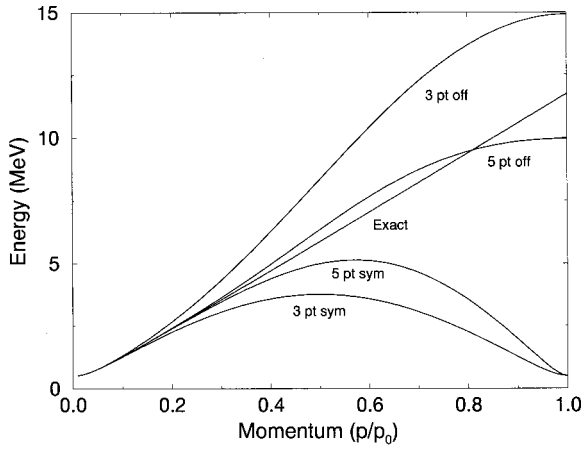

FIG. 1. Energy dispersion relations for the one-dimensional free-particle Dirac equation. The labeling (n pt sym) refers to a symmetric n point central difference, while (n pt off) refers to an offset n point backward-forward difference. The scaled momentum units are in $p_0=\pi/\Delta x$, the maximum momentum on the lattice.

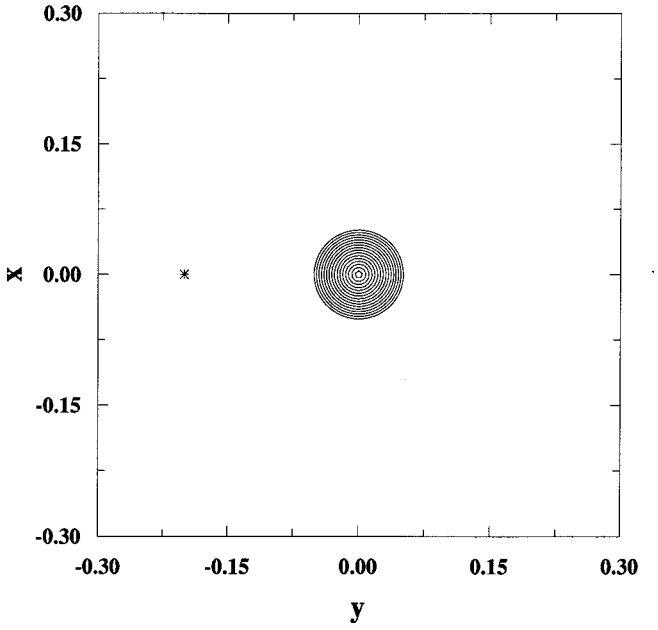

FIG. 2. Time-equal 0.00-a.u. Schrödinger equation solution on a 600×600 point lattice. The Pd^{46+} on Pd^{45+} collision is at 50.0 MeV/amu and zero impact parameter [radial distances (x,y) are in atomic units, 1.0 a.u. $=5.29\times10^{-9}$ cm].

Similar equations provide probabilities for the solution of Eq. (4).

III. RESULTS

Total inelastic probabilities for collisions of Pd^{46+} on Pd^{45+} are calculated by direct solution of the Schrödinger and Dirac equations on a two-dimensional Cartesian lattice. We employ a 600×600 point lattice with a uniform grid spacing of $\Delta x=\Delta y=0.001$ a.u., yielding a box size of 0.60 a.u. on each side. To avoid difficulties with representing the singular Coulomb potential on a numerical lattice of finite spacing, we introduce a soft-core parameter s such that

$$V(r)=-\frac{Z}{r}\rightarrow V(r)=-\frac{Z}{\sqrt{s^2+r^2}}. \tag{34}$$

For the 600×600 point lattice we choose $s=0.002$ a.u. Spurious wave reflection at the lattice boundary is eliminated through the use of exponential masking.

We present electron probability density plots as a function of time in Figs. 2 and 3 for a solution of the Schrödinger equation at an incident energy of 50 MeV/amu, corresponding to an incident velocity of 44.9 a.u. (or approximately $\frac{1}{3}$ the speed of light), and zero impact parameter. The initial position of the bare Pd^{46+} projectile is indicated by a star in Fig. 2 at $(x=0.00,y=-0.20)$, while the single electron Pd^{45+} target is centered in the box. After moving past the center of the box, the projectile is now located at $(x=0.00,y=+0.07)$ in Fig. 3. The electron probability density is almost equally centered about the projectile and target,

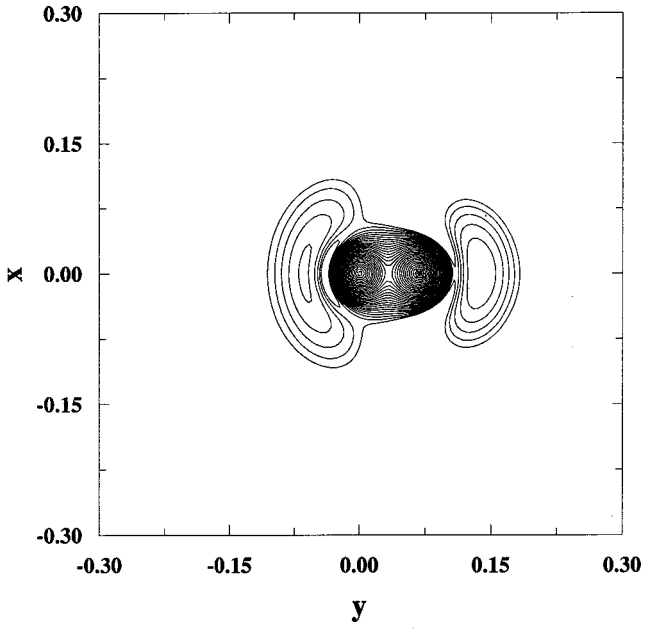

FIG. 3. Time-equal 0.09-a.u. Schrödinger equation solution on a 600×600 point lattice. The Pd^{46+} on Pd^{45+} collision is at 50.0 MeV/amu and zero impact parameter [radial distances (x,y) are in atomic units, 1.0 a.u. $=5.29\times10^{-9}$ cm].

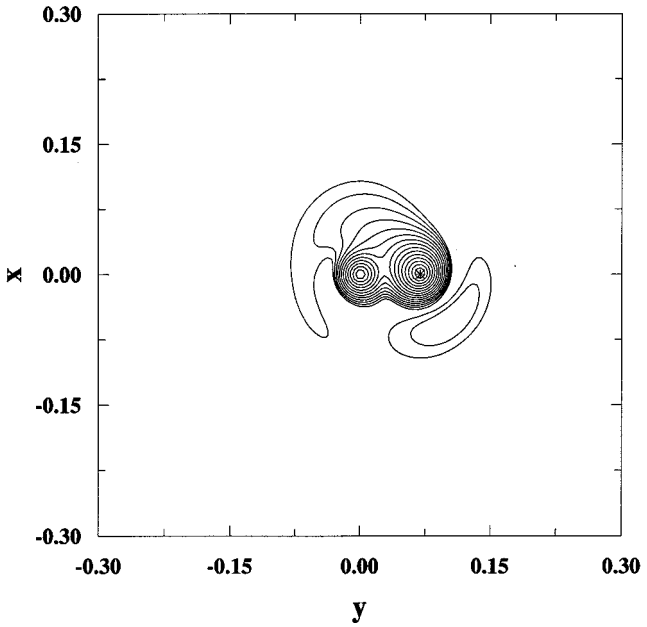

FIG. 4. Time-equal 0.09-a.u. two-component Dirac equation solution on a 600×600 point lattice. The Pd^{46+} on Pd^{45+} collision is at 54.4 MeV/amu and zero impact parameter [radial distances (x,y) are in atomic units, 1.0 a.u. $=5.29\times10^{-9}$ cm].

indicating substantial charge transfer. Out ahead of the projectile is a small ''hill'' of probability, indicating a small chance of binary electron knockout at twice the projectile speed. The time propagation is continued until the projectile reaches $(x=0.00,y=+0.20)$, at which time the inelastic probability from Eq. (31) is found to be 0.53.

We present electron probability density plots as a function of time in Figs. 4 and 5 for a solution of the Dirac equation at an incident energy of 54.4 MeV/amu, corresponding to an incident velocity of 44.9 a.u., and zero impact parameter. The two-component Dirac equation results are shown in Fig. 4 and the four-component Dirac equation results are shown in Fig. 5. Both relativistic solutions began at the same initial position of the bare Pd^{46+} projectile as shown in Fig. 2, and the results presented are at the same collision time and position as shown in Fig. 3. Somewhat more electron probability density is centered on the projectile than on the target, indicating more charge transfer in the relativistic case. When the time propagation is continued until the projectile reaches $(x=0.00,y=+0.20)$, the two-component Dirac inelastic probability is found to be 0.82, while the inelastic probability for the four-component solution is found to be 0.74.

Of peculiar interest are the small flows of electron probability density moving ahead and to the sides of the Pd^{46+} projectile in Figs. 4 and 5. Although the collision takes place at zero impact parameter, there is quite a noticeable reflection asymmetry about the $x=0$ axis for the two-component Dirac solution shown in Fig. 4. Although one might expect some small asymmetry due to numerical error, the same large asymmetry is found in the two-component Dirac solution on comparing calculations made with three-point backward-forward, five-point backward-forward, and even three-point central difference forms for the momentum operators. We attribute the change in the degree of reflection asymmetry in moving from the two- to four-component Dirac solutions as due to the asymmetric $\partial A_y/\partial x$ ''magnetic'' term in the respective nonrelativistic reductions found in Eqs. (8) and (12). In the two-component case, the asymmetric ''magnetic'' term acts directly on the spin 0 reduced

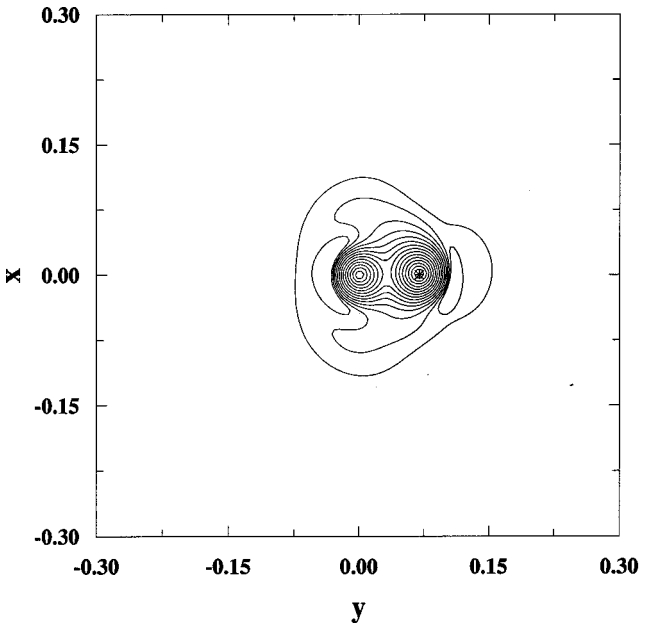

FIG. 5. Time-equal 0.09-a.u. four-component Dirac equation solution on a 600×600 point lattice. The Pd^{46+} on Pd^{45+} collision is at 54.4 MeV/amu and zero impact parameter [radial distances (x,y) are in atomic units, 1.0 a.u. $=5.29\times10^{-9}$ cm].

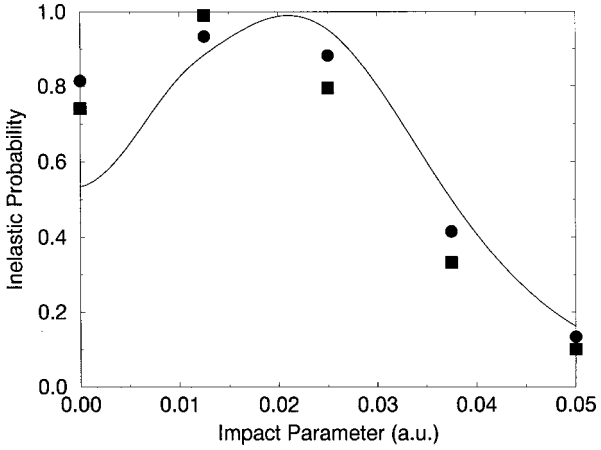

FIG. 6. Inelastic probabilities versus impact parameter for Pd^{46+} on Pd^{45+} collisions at the same incident ion velocity of 44.9 a.u. Solid line: Schrödinger equation solution, solid circles: two-component Dirac equation solution, solid squares: four-component Dirac equation solution.

wave function, while in the four-component case it acts to couple the spin $\frac{1}{2}$ components of the reduced wave function.

Extending both our Schrödinger and Dirac equation solutions to nonzero impact parameters, we present the total inelastic probability as a function of impact parameter in Fig. 6 at an incident ion velocity of 44.9 a.u. All the inelastic probability results are in good agreement at large impact parameters, but the two- and four-component Dirac results are substantially higher than the Schrödinger results at small impact parameters.

For a final comparison, we employ a 240×240 point two-dimensional lattice with a uniform grid spacing of $\Delta x=\Delta y$

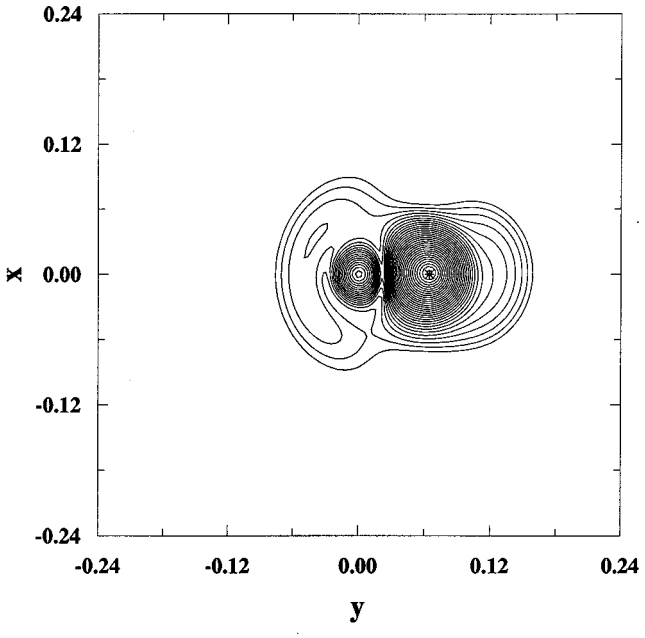

FIG. 7. Time-equal 0.09-a.u. four-component Dirac equation solution on a 240×240 point lattice. The Pd^{46+} on Pd^{45+} collision is at 54.4 MeV/amu and zero impact parameter [radial distances (x,y) are in atomic units, 1.0 a.u. $=5.29\times10^{-9}$ cm].

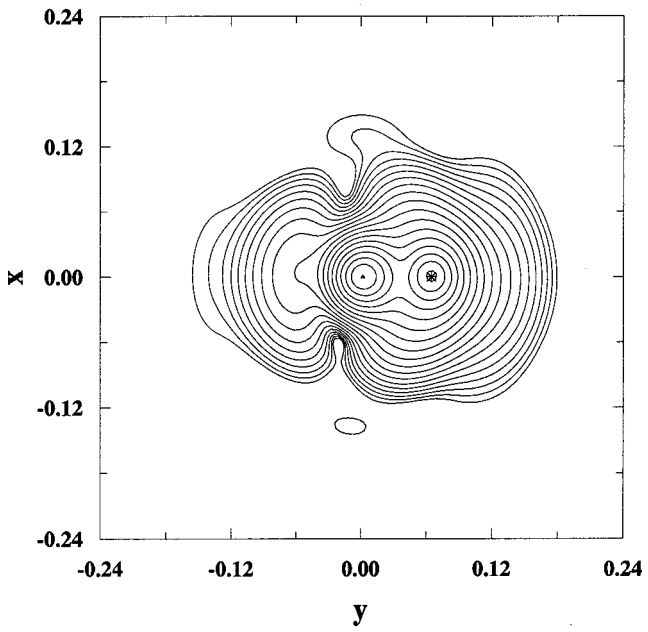

FIG. 8. Time-equal 0.09-a.u. four-component Dirac equation solution on a $240\times240\times240$ point lattice. The Pd^{46+} on Pd^{45+} collision is at 54.4 MeV/amu and zero impact parameter [radial distances (x,y) are in atomic units, 1.0 a.u. $=5.29\times10^{-9}$ cm].

$=0.002$ a.u. and a soft core parameter $s=0.004$. The four-component Dirac results are shown in Fig. 7 following a collision of Pd^{46+} on Pd^{45+} at an incident velocity of 44.9 a.u. and zero impact parameter. The time-dependent calculations for the four-component Dirac equation are then repeated on a full $240\times240\times240$ point three-dimensional lattice. The probability density in the $z=0$ plane is shown in Fig. 8 at the same point in collision time and position as found in Fig. 7. The collision dynamics in two and three dimensions are quite similar, even though the weaker binding for a Pd^{46+} on Pd^{45+} collision in three dimensions is reflected in a much larger spatial extent of the electron density cloud.

IV. SUMMARY

Ion-ion collision dynamics are studied by direct solution of the time-dependent Schrödinger and Dirac equations on an identical two-dimensional lattice. In the intermediate energy range, the nonrelativistic and fully relativistic inelastic probabilities for a Pd^{46+} on Pd^{45+} collision are found to be in good agreement at large impact parameters, but differ substantially at small impact parameters. When the ion-ion collision solutions of the time-dependent Dirac equation in two and three dimensions are compared, the evolution of the electron probability densities is found to be similar. This is in keeping with previous studies [13,14] comparing ion-atom solutions of the time-dependent Schrödinger equation in two and three dimensions. Based on these exploratory studies, it seems that ion-ion collisions may be readily carried out by direct solution of the time-dependent Dirac equation on a full three-dimensional lattice, although the computational effort is about four times that of the Schrödinger equation. The fact that this nonperturbative computational approach permits a

close examination of the short time collision dynamics, while at the same time providing cross sections for a variety of state-selective excitation and charge-transfer processes, remains its most appealing feature. However, we urge caution in extending these studies to examine relatively weak collision processes at high incident energies, where the choices that we have made for the energy dispersion relation, the nuclear potential, and the gauge for the projectile interaction must all be reevaluated.

ACKNOWLEDGMENTS

I would like to thank Dr. Francis Robicheaux, Dr. Jack Wells, and Dr. David Schultz for several useful discussions. This work was supported in part by the U.S. Department of Energy under Grant No. DE-FG05-96-ER54348 with Auburn University. Computational work was carried out at the National Energy Research Supercomputer Center in Berkeley, CA.

[1] J. Eichler and W. E. Meyerhof, in *Relativistic Atomic Collisions* (Academic, San Diego, 1995).
[2] U. Becker, N. Grun, and W. Scheid, J. Phys. B **16**, 1967 (1983).
[3] U. Becker, N. Grun, W. Scheid, and G. Soff, Phys. Rev. Lett. **56**, 2016 (1986).
[4] J. Thiel, A. Bunker, K. Momberger, N. Grun, and W. Scheid, Phys. Rev. A **46**, 2607 (1992).
[5] M. R. Strayer, C. Bottcher, V. E. Oberacker, and A. S. Umar, Phys. Rev. A **41**, 1399 (1990).
[6] J. C. Wells, V. E. Oberacker, A. S. Umar, C. Bottcher, M. R. Strayer, J. S. Wu, and G. Plunien, Phys. Rev. A **45**, 6296 (1992).
[7] J. C. Wells, V. E. Oberacker, M. R. Strayer, and A. S. Umar, Phys. Rev. A **53**, 1498 (1996).
[8] A. Belkacem and D. Ionescu, NERSC Annual Report No. LBNL-42920, 1999, p. 43.
[9] A. Kolakowska, M. S. Pindzola, F. Robicheaux, D. R. Schultz, and J. C. Wells, Phys. Rev. A **58**, 2872 (1998).
[10] A. Kolakowska, M. S. Pindzola, and D. R. Schultz, Phys. Rev. A **59**, 3588 (1999).
[11] M. S. Pindzola, Phys. Rev. A **60**, 3764 (1999).
[12] P. Gavras, M. S. Pindzola, D. R. Schultz, and J. C. Wells, Phys. Rev. A **52**, 3868 (1995).
[13] J. C. Wells, D. R. Schultz, P. Gavras, and M. S. Pindzola, Phys. Rev. A **54**, 593 (1996).
[14] S. Carlip, Phys. Rev. D **45**, 3584 (1992).
[15] A. Neagu and A. M. J. Schakel, Phys. Rev. D **48**, 1785 (1993).
[16] Y. Hosotani, Phys. Rev. D **51**, 2022 (1995).
[17] C. L. Ho and V. R. Khalilov, Phys. Rev. A **61**, 032104 (2000).
[18] U. W. Rathe, C. H. Keitel, M. Protopapas, and P. L. Knight, J. Phys. B **30**, L531 (1997).
[19] J. W. Braun, Q. Su, and R. Grobe, Phys. Rev. A **59**, 604 (1999).
[20] L. Susskind, Phys. Rev. D **16**, 3031 (1977).
[21] C. Bottcher and M. R. Strayer, Ann. Phys. (N.Y.) **175**, 64 (1987).
[22] C. Muller, N. Grun, and W. Scheid, Phys. Lett. A **242**, 245 (1998).
[23] O. Busic, N. Grun, and W. Scheid, Phys. Lett. A **254**, 337 (1999).
[24] R. L. Burden, J. D. Faires, and A. C. Reynolds, *Numerical Analysis* (Prindle, Weber, and Schmidt, Boston, 1978).